

Non-exponential decay in a RC circuit: unequal currents entering and leaving the capacitor

Frank V. Kowalski*

Physics Department, Colorado School of Mines, Golden CO. 80401 U.S.A.

(Dated: May 12, 2022)

The response of a resistor-capacitor circuit is shown to both decay non-exponentially and to have unequal currents flowing into and out of the capacitor. This is demonstrated using a variable air capacitor. A possible mechanism for the effect is illustrated in the decay a dielectric capacitor.

Capacitors are essential stand alone or inherent components of virtually every electronic system or device. Applications are in storing energy, filtering, signal coupling, noise suppression, sensors, oscillators, and probes of the microscopic structure of matter (dielectric spectroscopy is such an example).

The capacitor's response is often modeled using Kirchhoff's current and voltage laws. When applied in steady state these predict that the charges on the capacitor plates are equal and opposite and that exponential decay occurs in a RC circuit. The same current then flows into one terminal of the capacitor and out of the other.

However, such behavior is not typically found in a practical device. For example, non-exponential decay was first studied during the 1850's using Leyden jars and modeled with stretched exponential functions [1]. Non-ideal behavior is often associated with the dielectric used to increase capacitance [2, 3]. Other non-ideal effects are a result of the electronic properties of the conducting plates leading to a quantum treatment of capacitance [4]. Circuit simulation software typically accounts for non-ideal behavior with a lumped circuit model that includes an equivalent series inductance and resistance along with the capacitance.

Examples, shown below, demonstrate both that such decay is neither that of a stretched exponential nor of an exponential and that the currents flowing into and out of the plates are asymmetrical. In the context of dielectric spectroscopy, the decay behavior of a capacitor which contains a dielectric is then not necessarily completely indicative of the dielectric's relaxation, but can also be a function of the circuit design. The purpose here is to present data illustrating limitations of this steady state assumption when applied to RC decay rather than to generate a model that supports this data. Nevertheless, evidence of a potential mechanism, related to the binding of positive and negative charges on opposite capacitor plates [5, 6] is presented.

The majority of the results below utilize the circuit shown in the frame (b) inset of fig. 1. A mechanical switch couples and decouples the battery from the circuit. A variable air capacitor [7] set at 240 pF is charged to 19.8 V. The two channels of an oscilloscope[8] with 16 bit resolution at 10 MS/s are used to collect data. The

probes are set on a x10 scale with an input resistance 10M Ω and a capacitance of 15pF.

The currents through each resistor for $R_1 = R_2 = 47\text{K}\Omega$ are displayed in fig. 1. Frame (a) illustrates the full current scale over a duration of 4 time constants while the duration in frame (b) is over 18 time constants with a reduced current scale.

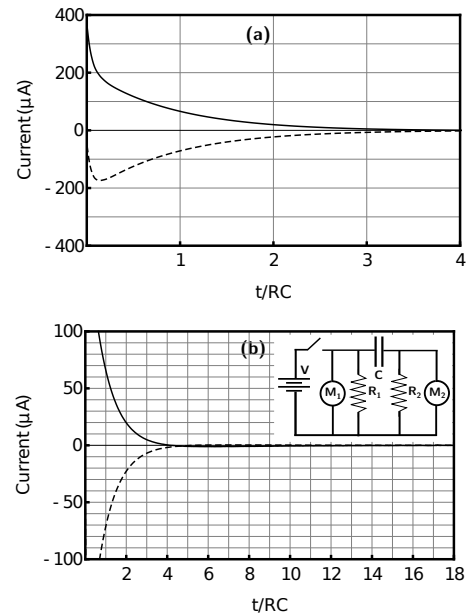


FIG. 1. The decay currents through R_1 (solid) and R_2 (dashed), respectively, as a function of time in time constant units. The circuit used is shown in the lower inset of frame (b). M_1 and M_2 represent the meters that measure the voltages (and therefore the currents from Ohm's law) across R_1 and R_2 .

The currents through the two resistors are given in fig. 2, again with $R_1 = R_2$, but on a finer voltage scale for different resistance pair values over 40 time constants in (a) and 18 in (b), (c), and (d). Four raw data results for each circuit are superimposed to illustrate repeatability of the data.

While the small differences in the currents through R_1 and R_2 on a time scale greater than two time constants are given in fig. 2, larger differences for shorter time scales are shown in fig. 3. The data are presented as a percent change in the currents flowing into and out of

* fkowalsk@mines.edu

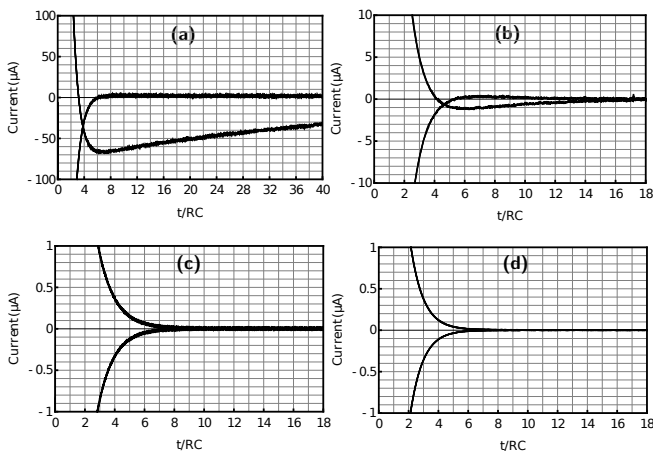


FIG. 2. Currents through R_1 and R_2 as in fig. 1 but for resistor pair values of $4.7\text{K}\Omega$, $47\text{K}\Omega$, $225\text{K}\Omega$, and $704\text{K}\Omega$ shown in frames (a), (b), (c), and (d), respectively.

the capacitor, $\Delta\text{Current}(\%) = (I_{R_1} + I_{R_2})/I_0$ where I_0 is the current through R_1 long after the circuit has been energized but before the decay. Again multiple traces for each value of the resistance are presented.

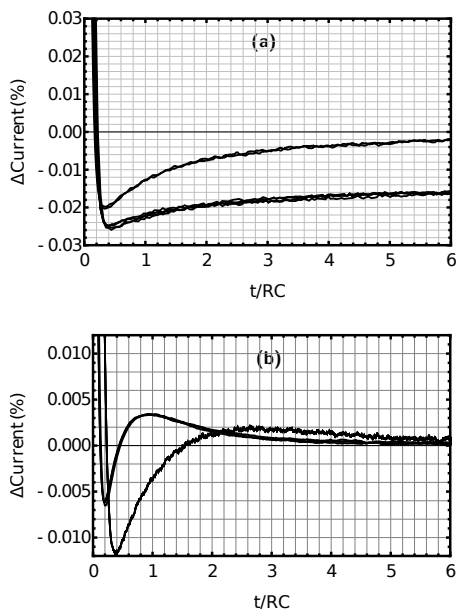


FIG. 3. The percent difference in current flowing into and out of the capacitor for resistor pair values of $4.7\text{K}\Omega$ (the lower trace in (a)), $47\text{K}\Omega$ (upper trace in (a)), $225\text{K}\Omega$ (the trace with the most negative minimum in (b)), and $704\text{K}\Omega$ (the remaining trace in (b)). All traces approach zero over longer time scales.

The mathematical form of the RC decay as a function of time is expected to be exponential and therefore is most often presented in a semi-log plot. However, since the current can oscillate, this is modified using the loga-

rithm of the absolute value of the current. The interpretation of such graphs is best illustrated using the currents shown in fig. 2 (b) and fig. 4 (b). The dips in the semi-log plots of 4 (b) correspond to the zero currents in fig. 2 (b). After going negative (reversing direction) the current then slowly approaches zero which is indicated in the semi-log plot by a downward slope.

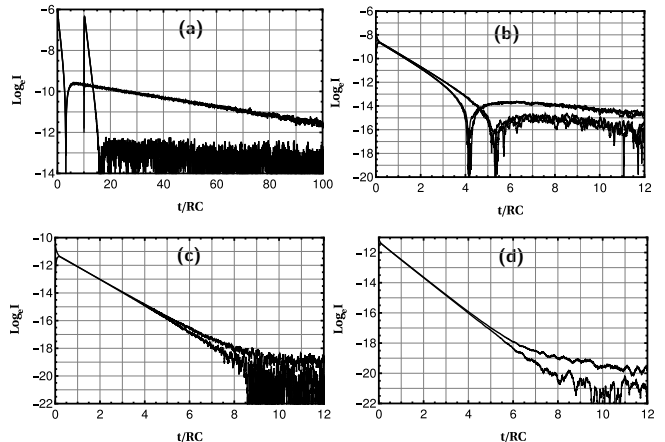


FIG. 4. Semi-log plots of $\log_e |I_{R_1}|$ and $\log_e |I_{R_2}|$ for resistor pair values of $4.7\text{K}\Omega$, $47\text{K}\Omega$, $225\text{K}\Omega$, and $704\text{K}\Omega$ are shown in frames (a), (b), (c), and (d), respectively. In each of these graphs the decay over the full variation of currents is displayed. In all frames I_{R_1} is the higher trace at $t/RC = 100$ in frame (a) and it is the higher trace at $t/RC = 12$ in frames (b), (c), and (d). For clarity the $\log_e |I_{R_2}|$ trace in frame (a) is delayed by ten time constants.

In such plots the absolute value of the current is never negative. The noise current that fluctuates about zero is always positive, yielding a noise baseline that is best illustrated by the $\log_e |I_{R_2}|$ current shown in fig. 4 (a).

The charge on each plate can be calculated by integrating the currents flowing into and out of the resistor connected to that plate. The net charge on the plates, $Q[t]$ varies as $dQ[t]/dt = I_{R_1} + I_{R_2}$, the functional form of which is shown in fig. 3.

Current oscillations in a circuit are typically indicative of an inductive component. Although the data do not accurately support a model of damped oscillations, a quarter period of such an oscillation can be estimated from figures. 1 (a) and (b) as the times when the current switches directions. The inductance required to generate such an oscillation in an LC circuit is of order 5 mH and 0.5 H for the data shown in figures. 1 (a) and (b), respectively. No such inductance is present in either the resistors, capacitor, or geometry used in the circuit.

The model perhaps most appropriate for exponential decay is that of the self capacitance associated with, for example, a charged sphere. The rate at which its charge decays through a resistor to infinity is proportional to charge on the sphere. However, the mutual capacitance associated with two such neighboring spheres adds an interaction term (in a typical derivation of exponential

decay in a RC circuit the mutual capacitance simply replaces the self capacitance of the one sphere model).

This interaction is associated with the attraction between induced positive and negative charges on the capacitor plates. Fig. 5 illustrates this effect by first presenting data in frame (a) for the charging and discharging of the circuit used in the previous figures. Note that the charging and discharging rates differ since the former involves only R_2 while the latter involves $R_1 + R_2$. Although not clearly discernible, the decay of the currents is similar to that shown in fig. 4 (d).

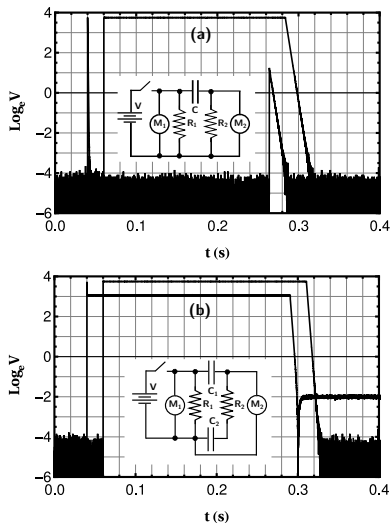


FIG. 5. Semi-log plots of $\log_e |V_{R_1}|$ and $\log_e |V_{R_2}|$ for resistor values of $R_1 = 2.2\text{K}\Omega$ and $R_2 = 158\Omega$ with capacitor values $C_1 = C_2 = 2\mu\text{F}$ (film metalized polypropylene axial capacitors). Both the switching of the battery into and then out of the circuit are shown. The circuits used to obtain the data are in the respective insets.

For clarity the $\log_e |V_{R_1}|$ traces in frames (a) and (b) of fig. 5 are delayed by 0.02 s from the time at which the switch is closed at $t = 0.04$ s. The $\log_e |V_{R_2}|$ trace of frame (a) is then shown to begin at $t = 0.04$ s and appears as a spike corresponding to the induced charge flowing to the right plate of C through R_2 .

The circuit in frame 5(b) isolates the right plate of

C_1 from ground potential using capacitor $C_2 = C_1 = C$. After the switch has been closed for multiple time constants, charge is induced on the plates of C_1 and C_2 . The potential on the right plates of C_1 and C_2 is reduced from that of the battery due to the voltage drop across C_1 created by this charge.

After the switch is opened the voltages on the left hand plates of C_1 and C_2 decay to ground potential. However, induced charge remains on the right hand plates as indicated by the non-zero voltage with respect to ground shown on the $\log_e |V_{R_2}|$ trace long after the switch has been opened. If, on the other hand, this negative induced charge on the right plate of C_1 flowed to the positive induced charge on the right plate of C_2 then V_{R_2} would be at ground potential. Although not observed in this dynamical system, such a ground potential on the right hand plates is predicted in the context of electrostatics [9, 10].

To quantify this persistent voltage (long after the switch is opened) for battery voltages $V_0 = 5, 20,$ and 40 V the ratio of this offset voltage to V_0 is measured to be -0.0037 ± 0.0005 , -0.0034 ± 0.0003 , and -0.0036 ± 0.0002 , respectively. This indicates a linear relation between the battery voltage and the voltage that persists on the capacitors due to the attraction between the charges induced on neighboring plates. This ratio for the air capacitor with $C_1 = C_2 = 120$ pF is measured to be -0.0023 ± 0.0002 for $V_0 = 12$. For such a measurement on the air capacitors the 10 G Ω input impedance of the voltmeter (Keysight 34465A) is needed to prevent the charge on the right hand plates of the C_1 and C_2 capacitors from decaying through the meter before a measurement can be made.

This attraction between opposite charges on the plates could reduce the decay rate from that of an exponential, becoming pronounced near the end of the decay. For example, the decreasing decay rate shown in frames (c) and (d) of fig. 4 may indicate such an effect. Systems that are modeled with a stretched exponential function may to some extent be influenced by the attraction between charges on the plates affecting the decay. Other possible examples are illustrated in systems with time constants much longer than those of fig. 3 (a) and (b) [11].

[1] R. Kohlrausch, “Theorie des elektrischen rückstandes in der leidener flasche,” *Ann. Phys.* **167**, 56–58 (2009).
 [2] Andrew K Jonscher, “Dielectric relaxation in solids,” *Journal of Physics D: Applied Physics* **32**, R57–R70 (1999).
 [3] Yuri Feldman, Alexander Puzenko, and Yaroslav Ryabov, “Dielectric relaxation phenomena in complex materials,” *Advances in Chemical Physics* **133**, 1 – 125 (2005).
 [4] T. Kopp and J. Mannhart, “Calculation of the capaci-

tances of conductors: Perspectives for the optimization of electronic devices,” *Journal of Applied Physics* **106**, 064504 (2009).
 [5] Brian Skinner and B. I. Shklovskii, “Anomalously large capacitance of a plane capacitor with a two-dimensional electron gas,” *Phys. Rev. B* **82**, 155111 (2010).
 [6] C. Berthod, H Zhang, A. F. Morpurgo, and T. Giamarchi, “Theory of cross quantum capacitance,” *Phys. Rev. Research* **3**, 043036 (2021).
 [7] Hammarlund model 2716-15.

- [8] Picoscope model 4262.
- [9] E. M. Purcell, (*Electricity and Magnetism Vol. 2*). (McGraw Hill College, 1985) p. problem 3.8.
- [10] D. J. Griffiths, (*Introduction to Electrodynamics*). (Prentice-Hall, 1989) pp. 120–121.
- [11] Justin L. Swantek, Tony D’Esposito, Jacob Brannum, and Frank V. Kowalski, “Dielectric relaxation affected by a monotonically decreasing driving force: An energy perspective,” *Journal of Applied Physics* **130**, 154101 (2021).